

Active Lower Order Mode Damping for the Four Rod LHC Crab Cavity

A. C. Dexter, G. Burt, R. Apsimon

^aEngineering Department, University of Lancaster, Lancaster LA1 4YW, United Kingdom

^bThe Cockcroft Institute, Sci-Tech Daresbury, Daresbury, Warrington, United Kingdom

Abstract

The high luminosity upgrade planned for the LHC requires crab cavities to rotate bunches into alignment at the interaction points. They compensate for a crossing angle near to $500 \mu\text{Rad}$. It is anticipated that four crab cavities in succession will be utilized to achieve this rotation either side of each IP in a local crossing scheme. A crab cavity operates in a dipole mode but always has an accelerating mode that may be above or below the frequency of the operating mode. Crab cavities are given couplers to ensure that unwanted acceleration modes are strongly damped however employing standard practice these unwanted modes will always have some level of excitation. Where this excitation has a random phase it might promote bunch growth and limit beam lifetime. This paper sets out a method for active control of the phase and amplitude of the unwanted lowest accelerating mode in the crab cavities. The paper investigates the level of suppression that can be achieved as a function cavity quality factor and proximity to resonance.

Keywords: Active damping; Crab cavity; HL-LHC; LHC

1. Introduction

This paper demonstrates by analysis and modeling the feasibility of applying active damping to the lowest unwanted acceleration mode in crab cavities as would be appropriate for the LHC luminosity upgrade. This paper sets out the configuration and timing enabling a Low Level RF (LLRF) control system to actively damp the unwanted mode.

A novel aspect of this paper is the implementation of a cyclic or multi-valued set point. An unwanted mode must be controlled by RF near its centre frequency by manipulation of the I and Q components. Excitation is at the bunch repetition frequency and a designer aims for this to have no harmonic relationship to the unwanted modes. The paper shows how a cyclic or multi-valued set point minimizes control action.

The planned LHC luminosity upgrade [1] will utilize compact crab cavities [2] to adjust the orientation of the proton bunches at certain interaction points (IP) so as to increase luminosity to a defined level that can be maintained throughout the bunch lifetime [3]. Maximum luminosity is achieved when

bunches are in perfect alignment. Depending on the luminosity leveling scheme utilized, perfect alignment might not be utilized until the bunch population has been depleted after many hours of operation. For the proposed optics, luminosity would be reduced by a factor of about four when there is no bunch alignment using a crab cavity. The precise reduction factor depends on the level of focusing achieved. The proposal for the luminosity upgrade is to have control of the crabbing angles at interaction points 1 (ATLAS) and 5 (CMS).

A crab cavity is a deflection cavity operated with a 90° phase shift [4] so that a particle at the front of a bunch gets a transverse momentum kick equal and opposite to a particle at the back of a bunch while a particle at the bunch center receives no transverse momentum kick. The overall effect is the application of an apparent rotation to the bunch. In this paper a transverse change in momentum for a bunch or a particle as it passes through a cavity will be referred to as a kick. A kick is the integral of the force with respect to time per unit charge. As protons at the LHC travel close to the speed of light, the kick divided by the velocity of light is a voltage and henceforth all kicks will be

40 expressed as a voltage.

41 The simplest scheme for controlling crabbing angles is a 79
42 global scheme as was applied at KEKB [5]. In such a scheme 80
43 only one crab cavity is required per ring. Once the bunch has 81
44 a crabbing angle it rotates one way and then the other way 82
45 with respect to its nominal path as it passes through succes- 83
46 sive quadrupoles. For a given transverse voltage in the crab 84
47 cavity the maximum angle of rotation is limited by the focusing 85
48 properties of the lattice. The lattice is arranged so that bunches 86
49 have the ideal crabbing angle at the interaction points. For the 87
50 LHC luminosity upgrade, studies have indicated that having the 88
51 bunch oscillating about its axis along the entire circumference 89
52 is unacceptable; for this reason the current proposal is to use a 90
53 local crabbing scheme [6].

54 For a local scheme, crab cavities would be located before 92
55 and after each of the two IPs so that the crab rotation can be 93
56 removed. Both sets of crab cavities are positioned in a location 94
57 of relatively high beta so as to minimize the voltage that must 95
58 be applied in order to get the appropriate rotation at the IP and 96
59 to cancel the rotation after the IP.

60 The highest bunch repetition rate at the LHC is 40.08 MHz 98
61 for 25 ns operation and 20.04 MHz for 50 ns operation, the crab 99
62 cavity needs to operate at a multiple harmonic of these frequen-100
63 cies. Crab cavities are currently being designed to operate at101
64 400.8 MHz which is the same frequency as the accelerating RF102
65 and is sufficiently low for non linearities of the crab kick along103
66 the length of the 80 mm long bunches to be acceptable with104
67 respect to machine performance [6].

68 A crab cavity invariably uses a dipole mode to provide the106
69 transverse momentum kick. All RF cavities which admit dipole107
70 modes must also admit longitudinal modes. A designer aims108
71 for a high R/Q value of the operating dipole mode and low109
72 R/Q values for other modes. The R/Q value for each mode is110
73 $1/(2\omega C)$, which is half the capacitive impedance and it deter-111
74 mines the level of interaction of that mode with bunches passing112
75 through the cavity. Here the shunt impedance is taken as the113
76 acceleration voltage squared divided by the dissipated power,114
77 V^2/P . Crabbing and deflecting cavities designed to operate in115

78 a dipole mode will always have one accelerating mode with an
79 R/Q value comparable with the dipole mode's R/Q . Typically
80 this mode has a frequency which is below that of the dipole
81 mode as would be the case for the compact four rod crab cav-
82 ity [7]. Design optimization of the four rod cavity reduced the
83 R/Q of the low frequency accelerating mode to less than 1/7
84 of the R/Q of the operating dipole mode. An innovative design
85 for the LHC crab cavity also exists where the acceleration mode
86 frequency is somewhat higher than the operating mode [8]. For
87 this and similar cavities the R/Q of the accelerating mode is be-
88 tween 1/2 and one 1/3 of the R/Q of the operating mode and
89 hence more damping is required.

Section 2 of this paper looks at the level of bunch by bunch
91 excitation that would exist in the Lowest Order Mode (LOM)
92 of the four rod crab cavity when strongly damped with an ex-
93 ternal Q-factor, Q_e of 100 and for the anticipated LHC bunch
94 structure. This would often be referred to as the sum wake.

Section 3 proposes active damping with a feed forward con-
95 troller as a method to further reduce longitudinal dispersion of
96 bunches. Feed forward has been demonstrated experimentally
97 on accelerating cavities as a means of compensating beam load-
98 ing [9], although this paper outlines how such a scheme could
99 be used for compensating excitation of unwanted longitudinal
100 modes in deflecting cavities. Active damping has been investi-
101 gated previously for mixed higher order modes in a supercon-
102 ducting cavity [10]. The paper claimed some level of success
103 however the damping was not sufficient over a range of modes
104 to warrant implementation at CEBAF. The expected level of
105 damping achievable for the four rod LHC crab cavity is much
106 higher by virtue of the fact that the active damping control sys-
107 tem can be optimized to eliminate excitation in a single mode.
108 Damping the acceleration mode of the crab cavity to a Q_e of
109 100 without compromising the operating mode is technically
110 challenging. It is hoped that the application of active damping
111 will allow the level of passive damping to be reduced.

Section 4 simulates the effectiveness of active damping at
eliminating variations in longitudinal acceleration after gaps
in the LHC bunch structure. Results presented in this section

116 are again for the case when the acceleration mode is strongly
 117 damped with a Q_e of 100. This is the required level of damping
 118 in the absence of active damping.

119 Section 5 firstly considers active damping with the same con-
 120 trol parameters used in section 4 for the case when Q_e is in-
 121 creased to 300. As the quality factor is increased it becomes in-
 122 creasingly unlikely that the acceleration mode could be driven
 123 to become resonant. Covering a worst case scenario, this sec-
 124 tion shows that satisfactory active damping of the accelerating
 125 mode can be achieved even when it has moved to become reso-
 126 nant with the bunch repetition frequency.

127 Section 6 considers active damping performance with mod-
 128 erate detuning and significant measurement errors. After the
 129 consideration of measurement errors it is apparent that even
 130 a relatively poor estimate for the feed forward term still gives
 131 greatly improved damping performance with respect to the case
 132 without control.

133 Calculations and numerical simulations reported in this pa-
 134 per have been obtained by integration of the envelope equa-
 135 tions [11] and the model is described in the appendix. The en-
 136 velope equations are also used to model the output circuit of the
 137 power amplifier. This assumes the amplifier has an output cav-
 138 ity or tank circuit as would be the case for all high power, high
 139 efficiency amplifiers. Input parameters for the model include
 140 measurement errors, latency in the control system, microphon-
 141 ics and bunch charge fluctuations. The feed forward control
 142 scheme that has been proposed eliminates issues with latency
 143 (time delays). Solutions of the envelope equations with no mea-
 144 surement delays give the required feed forward drive power.

145 2. Mode excitation with no damping

146 A cavity mode voltage $V(t)$ can be referenced to its center
 147 angular frequency ω in terms of its in phase and quadrature
 148 components as

$$149 \quad V(t) = \Re \left[(A_r + jA_i) e^{-j\omega t} \right]. \quad (1)$$

Increments for the in phase and quadrature parts of the phasor

induced by a bunch of charge q passing through the cavity with
 RF phase α are given by

$$\delta A_r = \frac{q\omega}{2} \left(\frac{R}{Q} \right) \cos \alpha \quad (2)$$

and

$$\delta A_i = \frac{q\omega}{2} \left(\frac{R}{Q} \right) \sin \alpha. \quad (3)$$

When the unwanted accelerating mode frequency of a crab
 cavity is close to a multiple of the bunch repetition frequency
 then the phase α varies slowly in time and large voltages accu-
 mulate in the cavity.

Excitation within a bandwidth is referred to as resonant and
 the voltage moves in phase with the excitation. For modes
 with high loaded Q -factors, Q_L , and when a multiple of the
 bunch repetition frequency is not within several bandwidths of
 the cavity's natural frequency then the final voltage settles be-
 tween quadrature and anti-phase to the kick being provided by
 the bunches. Figure 1 shows the cavity voltage phase before and
 after the passage of a bunch when not excited near to resonance;
 this is the case of most interest as one designs cavities to avoid
 on resonance excitation of unwanted modes. Between bunches
 the mode phasor rotates and decays to its initial state. Close
 examination of the phasor diagram reveals the bunch initially
 sees a small acceleration followed by a stronger deceleration;
 the voltage has a small decrease followed by a larger increase.
 This means that the field induced in the mode tends to stretch a
 bunch; which is undesirable.

In order to limit beam induced accelerating voltages in the
 crab cavity a coupler is used which extracts power from the
 unwanted acceleration mode but rejects power from the oper-
 ating dipole mode. This coupler requires a notch filter if the
 acceleration mode's frequency is below the dipole mode and a
 simpler high pass filter if the acceleration mode's frequency is
 well above the dipole mode frequency.

If conditions allow large voltages to develop in an accel-
 erating mode then depending on the loaded Q factor of the
 mode and the frequency offset from the operating dipole mode

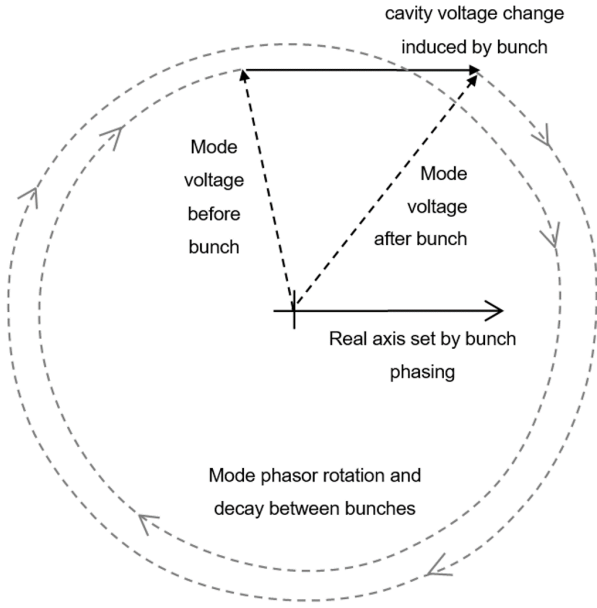


Figure 1: Off resonant excitation of a mode.

then significant power can be extracted from the beam and this power must exit the cavity through the coupler.

The voltage kick that acts on a bunch is the energy change ΔU of the cavity associated with the voltage increment divided by the bunch charge. From Eqs. 2 and 3 one can show

$$\frac{\Delta U}{q} = A_r \cos \alpha + A_i \sin \alpha + \frac{q\omega}{4} \left(\frac{R}{Q} \right) \quad (4)$$

where $A_r \cos \alpha + A_i \sin \alpha$ is the field in the cavity at the instant that the bunch arrives. From Eq. 4 one sees that it is possible to design a LLRF system that puts a small field in the cavity that accelerates the bunch as it approaches. The field then changes direction as the bunch deposits its image charge. The field then retards the bunch as it leaves. In this way a LLRF system can be designed so that bunches never receive a net voltage kick. With respect to Figure 1 this would be the case where the mode vectors before and after are symmetrical about the imaginary axis. It should be noted that if the unwanted mode frequency is exactly halfway between resonant frequencies then acceleration is equal to deceleration without a LLRF correction. A phasing which accelerates and then decelerates can stretch the bunch hence optimizing for zero kick is not necessarily the best control strategy for beam lifetime. Whilst this option will be in-

vestigated, the paper also investigates strategies where one only aims to give every bunch the same kick; for example, acceleration cavities are usually phased to compress bunches. With respect to Figure 1 achieving compression requires the cavity accelerating voltage to be falling as the bunch arrives hence the mode's phasor would be in the fourth quadrant.

In the absence of a LLRF system, or when an unwanted mode is damped and provided that bunches arrive continuously without gaps then a steady state voltage will become established for the unwanted mode. In this situation the phase advance and voltage damping between bunches is perfectly reset by the arrival of the next bunch. This pseudo steady state is synchronized to the bunch arrival times and not the mode frequency. This must be the case as the only drive frequency for the mode in the absence of a LLRF system is at the bunch frequency. The steady state mode vector prior to the arrival of a bunch and in the absence of RF control is derived in the next paragraph.

In the absence of beam loading the voltage $V(t)$ in a cavity evolves according to

$$\frac{d^2 V}{dt^2} + \frac{\omega_c}{Q_L} \frac{dV}{dt} + \omega_c^2 V = 0 \quad (5)$$

where ω_c is the instantaneous cavity frequency and Q_L is the loaded Q factor. Letting the time between bunches be Δt_b then the change in cavity voltage between bunches is determined as $V \rightarrow V e^z$, where

$$z = - \left[1 + j \sqrt{4Q_L^2 - 1} \right] \frac{\omega_c \Delta t_b}{2Q_L}. \quad (6)$$

Expressing the cavity voltage increment from a bunch determined from Eqs. 2 and 3 simply as δV then the condition for steady state is that $V(t) = V(t + \Delta t_b) = [V(t) + \delta V] e^z$. Solving $V = (V + \delta V) e^z$ gives

$$V = \frac{\delta V}{e^{-z} - 1}. \quad (7)$$

In Eq. 7 as before and without loss of generality the absolute phase of the kick can be chosen as zero so the phase of the cavity is determined by the term that multiplies δV . Defining

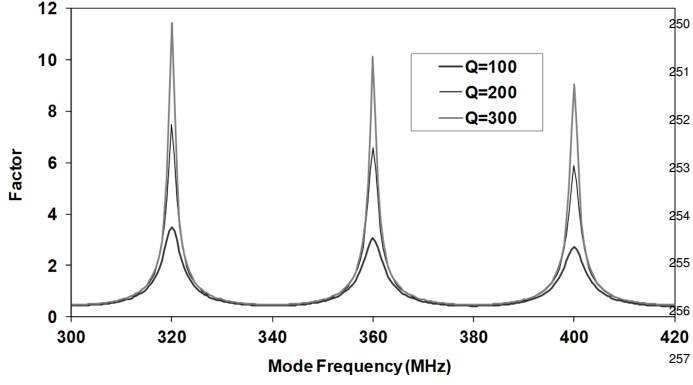


Figure 2: Cavity voltage magnitude just before the bunch arrives as function of mode frequency.

$$b = \frac{\omega_c \Delta t_b}{2Q_L} \quad (8)$$

and

$$\theta = \omega_c \Delta t_b \sqrt{1 - \frac{1}{4Q_L^2}} \quad (9)$$

then the phase of the cavity field at the instant before the bunch arrives is given by

$$\phi_V = -\tan^{-1} \left(\frac{\sin \theta}{\cos \theta - e^b} \right). \quad (10)$$

The magnitude at the same instant is determined as

$$|V| = \frac{|\delta V| e^{\frac{b}{2}}}{\sqrt{2(\cosh b - \cos \theta)}}. \quad (11)$$

Note that the steady state voltage does not depend on the starting voltage $V(0)$ or the relative phase of the first bunch.

Figure 2 plots the factor multiplying of δV in Eq. 11.

It is known [11] that the voltage in a mode only becomes large when the mode frequency is an integer multiple of the bunch frequency. For Figure 2 these peaks are shown at 8, 9 and 10 times the higher bunch frequency of 40.08 MHz. For the compact 4 rod cavity design [6] the LOM has been positioned at 374 MHz but can be altered during design by a few MHz without affecting the performance of the operating mode.

Figure 2 shows that with a bunch frequency of 40.08 MHz then strong damping for the mode is unnecessary provided there is no chance of it shifting by 14 MHz to get to 360 MHz.

a bunch frequency of 20.04 MHz there are double the number of resonances with one occurring at 380 MHz. The requirement now becomes that the mode must not shift by 6 MHz. For a typical superconducting cavity such a large shift is impossible without a significant deformation of the cavity requiring a very large force. The cavity is designed to be sufficiently stiff for deformation from Lorentz force detuning to be less than 1 MHz. From Eq. 6 detuning due to loading is given as $f_0 \left(1 - \sqrt{1 - 1/4Q_L^2}\right)$ and for $Q_L \sim 100$ this gives a tiny shift of just 5kHz. One remaining concern is detuning caused by mechanical deflection and deformation of the couplers and this requires further study.

For the LHC crab cavity, the voltage in the unwanted acceleration mode voltage will need to be kept very small at all times to meet stringent limits on the longitudinal impedance of 0.2 M Ω per cavity [12]. Typically this would be guaranteed by having a coupler that strongly couples to the unwanted mode thereby extracting any power that the mode takes from the beam. Strong damping is only needed for mode frequencies close to a multiple of the bunch frequency. For most of the HOMs and potentially the LOM (lower order mode) there is an engineering uncertainty in the thermal contraction process and the tuning process with respect to frequency shifts. It is therefore necessary for all modes, unpredictable in this way, (and which cannot be independently tuned) to be sufficiently damped. This means that for the LOM one needs testing and modeling to understand how its frequency might shift after manufacture during processing, cooling and then tuning of the operating mode.

With respect to establishing a controller to reduce or eliminate kicks from the accelerating mode it is useful to think about evolution of the cavity phasor as has been illustrated in Figure 1. The phase reference is best referred to bunch arrival in which case $\alpha = 0$ in Eqs. 2 and 3 setting the voltage increment along the real axis. Eqs. 10 and 11 now give the cavity phasor the instant before the kick.

If the mode is resonant with bunch frequency then the starting phasor is on the positive real axis. For frequencies which are off resonance and for high loaded Q factors, the in-phase

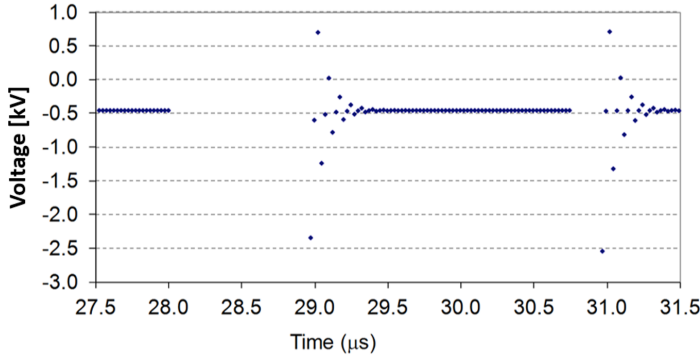


Figure 3: Voltage kicks to successive bunches $Q_e = 100$ with no active control.

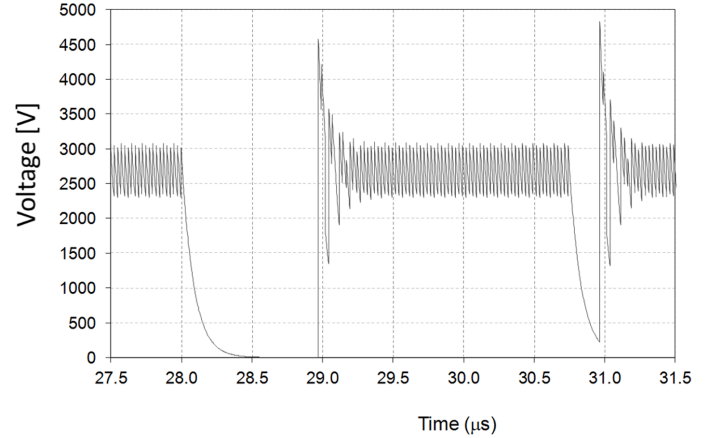


Figure 4: Cavity mode voltage with no active control, $Q_e = 100$.

288 voltage before the bunch arrives tends to $-\delta V/2$ and goes to
 289 $+\delta V/2$ as the bunch passes through the cavity while the quadra-
 290 ture voltage can become significant when the bunches are not
 291 in anti-phase.

292 The steady state condition of Eqs. 10 and 11 becomes upset
 293 whenever there are missing bunches in the bunch train. The
 294 LHC has a lot of missing bunches, there are small gaps of 8
 295 missing bunches associated with filling the SPS from the PS.
 296 There are larger gaps of either 38 or 39 bunches associated with
 297 filling the LHC from the SPS. Finally there is a very large gap
 298 of 102 bunches which is required for dumping the LHC beam.

299 Ordinarily after a gap, bunches get kicks that are substan-
 300 tially different to the kicks they would receive at steady state.
 301 Figure 3 shows successive voltage kicks for bunches arriving
 302 24.95 ns apart. A bunch train finishes at 28 μs , this is followed
 303 by a gap of 38 bunches ($\sim 1 \mu s$), then a train of 72 bunches,
 304 then a gap of 8 bunches (~ 200 ns) then a new train.

305 These results are from a simulation that integrates the
 306 envelope equations¹ but incorporates all the details of the
 307 LHC bunch structure. In this case the LOM frequency was
 308 374.08 MHz, its R/Q was 124.4 Ω , its external Q factor was
 309 100 and the bunch charge was 32 nC. The intrinsic Q factor, Q_0
 310 for superconducting cavities is invariably well over 10^6 hence
 311 the loaded Q factor can be regarded as being the same as the
 312 external Q factor throughout this paper. In Figure 3 the first
 313 5 voltage kicks after the long gap are -2539 V, -463 V, 717 V,
 314 -1315 V and -458 V; the settling value is -451.4 V.

¹see appendix

Beam power extracted by the crab cavities has to be added
 again by the acceleration cavities. As 12 crab cavities might be
 needed on each beam then the acceleration cavities must replace
 about 450 V of lost voltage per bunch due to the LOM. For an
 LHC current of 1A this amounts to 450 W. Clearly the mode
 couplers on each of the crab cavities in this case need to extract
 this amount of power.

Figure 4 shows simulated results for voltage in the cavity's
 unwanted acceleration mode corresponding to a train of 72
 bunches after a gap of 38 bunches and followed by a gap of
 8 bunches. When the mode has no initial voltage then a bunch
 charge of 32 nC then will excite an initial voltage of 4678 V
 as would be expected from knowledge of the R/Q , the bunch
 charge and the mode frequency. The fine structure in Figure 4
 is the exponential decay of the field after each bunch.

A problem with having differing kicks for different bunches
 is that where the main RF system is unable to respond suffi-
 ciently quickly to individual bunches then displaced bunches
 will not be at the optimum phase for acceleration and conse-
 quentially will have increased losses. Initially the losses will be
 from the leading bunches. Once charge is lost from the leading
 bunches the effective gap become larger and uneven kicks are
 then applied to bunches coming later in the train.

In section 3 two opportunities offered by active damping are
 considered. Firstly, to control the amplitude and phase of the
 unwanted acceleration mode so it is at the steady state point

whenever a bunch arrives thereby compensating for gaps in the bunch train. Good compensation can be achieved even with very small amounts of power. Secondly, to use RF power to move the in phase voltage back to $-\delta V/2$ whilst maintaining the quadrature voltage at the steady state point. This strategy ensures every bunch gets zero net kick. The amount of power required depends on how far the steady state point is from $-\delta V/2$.

3. Control strategy

An idealized LLRF system that might be used for active damping of an unwanted mode is shown in Figure 5.

The RF system needed to drive the mode needs to operate close to the mode's natural frequency so as to minimize power usage. Overall excitation of an unwanted mode is always at a frequency close to a harmonic of the bunch repetition frequency. This is composed of a driven oscillation near to the unwanted mode frequency plus potentially large phase jumps caused by bunches that moves the mode phase advance close to a multiple of 2π with respect to the bunch frequency. Active damping can be applied for any frequency of the unwanted mode with a conventional LLRF system. When the mode frequency differs from the bunch excitation frequency and the RF oscillator is centered on the mode frequency then active damping requires a new set point to be determined after each bunch has passed through the cavity. Effectively the LLRF system has to acknowledge that part of the phase advance per cycle is being provided by the beam. Stated another way, when a bunch passes through the cavity there is a jump in the phase. If the RF system driving the mode to a set voltage at the instant of each bunch has provided the correct amplitude and phase then the error term that corrects the RF after the bunch needs to remain almost the same. The jumps in the set points are just following expected phase changes caused by bunches. The set point is an IQ vector. Each new set point is calculated by a simple vector addition after each bunch has passed through the cavity based on the best estimate for the mode phase. The nominal vector change for the set point is calculated from the bunch repetition frequency and the best estimate for the mode frequency.

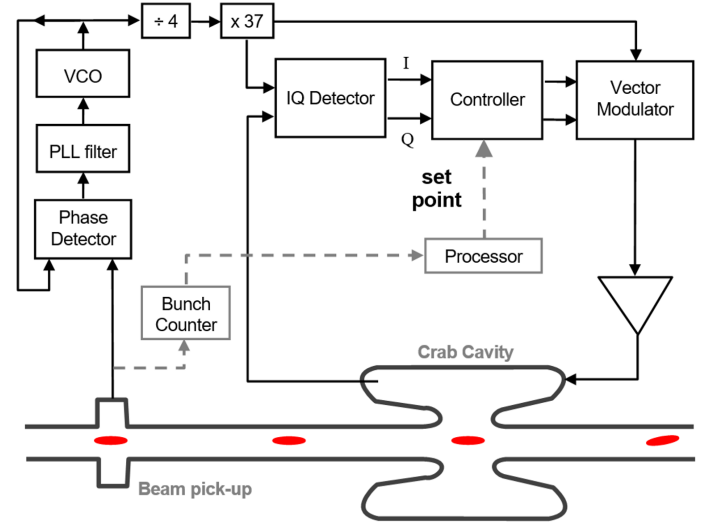


Figure 5: LLRF system controlling a cavity mode.

Because the mode is heavily damped control is relatively insensitive to errors in estimating the mode frequency.

The set point for the RF system is set after each bunch according to the algorithm

$$\begin{aligned} A_r(i) &= |V| \cos(\phi_V + \theta_i) \\ A_i(i) &= |V| \sin(\phi_V + \theta_i) \end{aligned} \quad (12)$$

where $A_r(i)$ and $A_i(i)$ are the in-phase and quadrature set point voltages for the mode with respect to the synthesized clock. $|V|$ and ϕ_V are the steady state amplitude and phase as defined previously in Eqs. 10 and 11 and θ_i is the expected RF phase for the next bunch.

For an arbitrary LOM frequency, there could potentially be an infinite number of set points, thus for clarity the simulations presented here use a LOM frequency such that only 3 set points are required. This means that θ_i in Eq. 12 cycles through three values and the exact LOM frequency which provides 3 set points is 374.08 MHz. The RF oscillator does not need to be at the exact centre frequency of the mode as the amplifier has a bandwidth and its precise frequency is determined by the controller correcting the phase, i.e. the vector modulator can add or subtract a frequency from the oscillator. The RF oscillator frequency for the unwanted mode would typically be generated from the bunch repetition frequency using an integer

399 divide PLL. For the example frequency of 374.04 MHz, synthe-437
400 sis is by dividing the bunch repetition frequency of 40.08 MHz⁴³⁸
401 by 3 and then multiplying by 28. Locking the drive frequency⁴³⁹
402 to a rational multiple of the bunch frequency forces the phas-⁴⁴⁰
403 ing between bunches and the LOM to maintain a predictable⁴⁴¹
404 advance. In this case the LOM does nine and a third cycles be-⁴⁴²
405 tween bunches hence the set points cycle after three bunches or⁴⁴³
406 28 LOM cycles. The bunch phase is predictable from the main⁴⁴⁴
407 timing system and hence a dedicated beam pick up shown in⁴⁴⁵
408 the left hand side of Figure 5 is unlikely to be needed; although⁴⁴⁶
409 it may be useful as a reference. The phase and amplitude of the⁴⁴⁷
410 unwanted LOM in the crab cavity is irrelevant except at the in-⁴⁴⁸
411 stant that bunches pass through the cavity. Here the amplitude⁴⁴⁹
412 and phase of the cavity would be measured with respect to the⁴⁵⁰
413 steady synthesized clock at 374.08 MHz. ⁴⁵¹

414 Each new set point is chosen so that when the next bunch⁴⁵²
415 arrives in the cavity it either ⁴⁵³
416 (a) has the steady state amplitude and phase ⁴⁵⁴
417 or ⁴⁵⁵
418 (b) has an amplitude and phase that gives zero bunch kick. ⁴⁵⁶

419 For a continuous train of bunches the set point moves by an⁴⁵⁷
420 amount almost equal to the amount that each bunch shifts the⁴⁵⁸
421 amplitude and phase of the mode. This means that for case (a)⁴⁵⁹
422 above the LLRF system does not need to deliver power unless⁴⁶⁰
423 there is a drift in the mode's natural frequency and for case (b)⁴⁶¹
424 only a small amount of power is delivered. For a continuous⁴⁶²
425 bunch train the set point cycles increments by the same vector⁴⁶³
426 for each bunch, however when there is a gap in the bunch train⁴⁶⁴
427 the next set point depends on the number of missing bunches.⁴⁶⁵
428 The nature of the controller shown in Figure 5 must be cho-⁴⁶⁶
429 sen with respect to the timescale over which corrections must⁴⁶⁷
430 be made. If corrections are to be made on every bunch then⁴⁶⁸
431 the correction must be made in 25 ns. If the correction is to⁴⁶⁹
432 be made during the short gap of 8 bunches there is a period of⁴⁷⁰
433 200 ns in which to make the correction. For an accelerator envi-⁴⁷¹
434 ronment making feedback corrections for individual bunches in⁴⁷²
435 25 ns is probably impossible. Analog corrections within 200 ns⁴⁷³
436 are possible but digital control on this timescale is challenging.⁴⁷⁴

For the damping of the unwanted acceleration mode, most of
the control action would be driven as feed forward corrections
by manipulation of the set point vector additions. During an
8 bunch gap the controller needs to rotate the cavity phasor to
a point near to where it should have been had the bunches not
been missing. If the new set point is written to an analogue con-
troller as the last bunch enters, then given that the rotation is less
than π a bandwidth of a few MHz is sufficient for the new set
point to be achieved on the correct timescale. When set points
are chosen optimally then feedback corrections become mini-
mized. At the LHC the charge of every bunch would be known,
its time of arrival in the cavity can be accurately predicted and
hence its action on a low frequency accelerating mode can also
be accurately predicted. In order to make a correction therefore
the control system must send a predetermined amount of charge
into the cavity at the correct phase over a number of RF cycles
to achieve each new set point. Variations in bunch charge and
detuning of the mode would require an element of feedback.

Optimal algorithms for the feed forward controller and a
methodology have yet to be developed. One simple method
to determine the feed forward power is to use the results of a
simulation employing a high gain proportional controller with
no delays in its action. The power that it predicts would then
be the power that is used in the real controller. Of course one
still needs accurate synchronization for the application of this
power. As the unwanted acceleration mode is certain to have a
very low external Q factor then feedback to compensate for fre-
quency drift of the mode is not critical in the way that it would
be for the operating mode in a typical accelerating cavity. The
analysis in the following section uses a high gain proportional
controller (no integral term) with minimal delay. When the
drive power that this controller predicts is regarded as the input
to the real cavity then the mode amplitude, the mode phase and
bunch kicks would be nominally the same as the predictions.
The feed forward term coming from the simulation is based on
expected bunch charge and mode center frequency. As some
variation is expected, the feed forward contribution might be
supplemented with a feedback term based on errors for the pre-

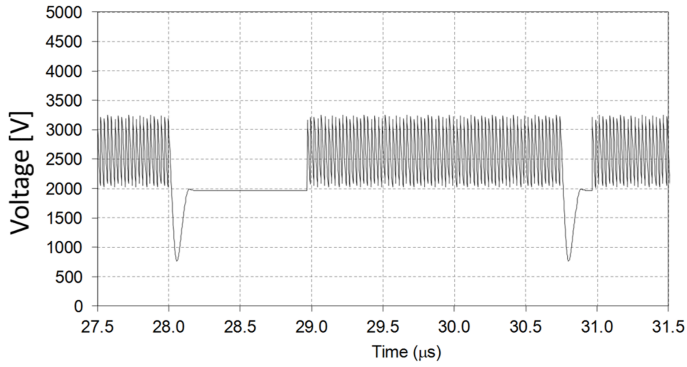


Figure 6: Mode voltage using active control with gain = 1500, $Q_e = 100$, set point = no control steady state point.

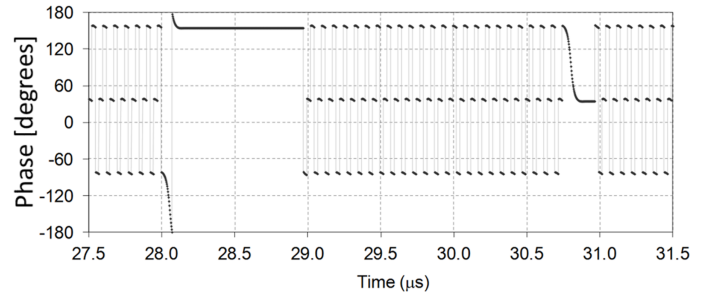


Figure 7: Mode phase when bunch at cavity center using active control with gain = 1500, $Q_e = 100$, set point = no control steady state point.

475 vious bunch train. The feedback period might be the 80 buckets
 476 associated with the PS fill, the 270/271 buckets associated with
 477 the SPS fill or an entire LHC train.

478 For these simulations the new control set point is given to
 479 the controller on the time iteration after the bunch has passed
 480 through the cavity. (The software that has been developed has
 481 the option to consider any delay greater or equal to one time
 482 iteration). The time iteration chosen for the simulations was the
 483 period of the unwanted mode.

484 For a real system the set point is compared to a measured
 485 value of the cavity voltage. The measurement system which
 486 can be regarded as part of the IQ detector shown in Figure 5
 487 will have a bandwidth. The software includes a measurement
 488 bandwidth but as code is being used to determine the feed for-
 489 ward term the bandwidth has been set very high.

490 4. Active damping performance

491 Figures 6, 7, 8 and 9 plot computed mode voltage amplitude,
 492 phase and RF power and the voltage kick applied to the beam
 493 respectively for the proposed controller. The controller is fully
 494 feed forward, but the I and Q components of the drive are com-
 495 puted from a high gain proportional controller using cyclic set
 496 points to keep the amplitude and phase at the point to which
 497 they are naturally damped.

498 The slew rate of the amplifier is determined by the propor-
 499 tional gain and the amplifier bandwidth. The amplifier band-
 500 width was chosen as 50 MHz and the proportional gain taken

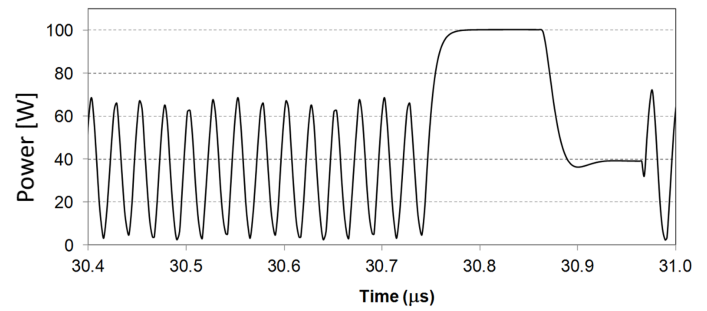


Figure 8: RF power using active control with gain = 1500, $Q_e = 100$, set point = no control steady state point.

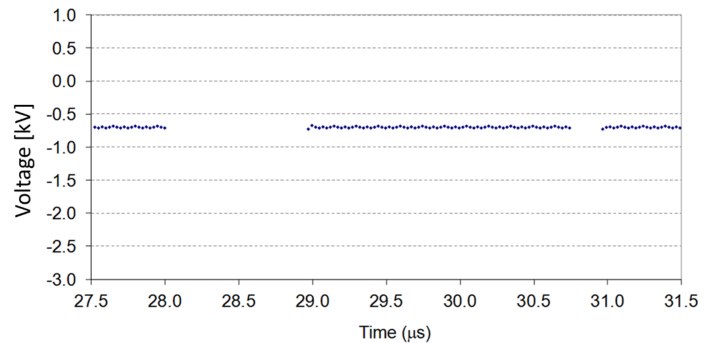


Figure 9: Bunch kicks using active control with gain = 1500, $Q_e = 100$, set point = no control steady state point.

501 sufficiently high for the new set point to be easily achieved
 502 within the short 8 bunch gap of 200 ns. Comparing Figure 6
 503 with Figure 4 the voltage now starts in its steady state pattern
 504 for the bunch train. A voltage level is set during the gap of miss-
 505 ing bunches to ensure that the cavity is at the correct amplitude
 506 and phase for the next bunch.

507 Figure 7 shows the three phases associated with chosen fre-
 508 quency ratios. The phase is measured with respect to the mas-
 509 ter oscillator running at the center frequency of the LOM (phase
 510 with respect to bunch arrival times is of course tending to a con-
 511 stant value). In this particular case a phase of 155° is set during
 512 the long gap and a phase of 38.4° is set during the short gap
 513 in accordance with the expected time of arrival of the follow-
 514 ing bunch. For this simulation the maximum power was con-
 515 strained to 100 W which is just below the peak demand from
 516 the controller during gaps.

517 Figure 8 initially shows the required power towards the end
 518 of a train of 72 bunches. Close examination of the data indi-
 519 cates that bunches arrive as the power dips to zero. The last⁵³⁹
 520 bunch in the train arrives at $30.74 \mu\text{s}$. After $30.74 \mu\text{s}$ the figure⁵⁴⁰
 521 shows the power used to reset and maintain a new amplitude⁵⁴¹
 522 and phase in anticipation of the next bunch during a short δ ⁵⁴²
 523 bunch gap. The new level is achieved at $30.9 \mu\text{s}$ after which the⁵⁴³
 524 power gets reduced to 40 W in order to maintain the set point.⁵⁴⁴
 525 The figure shows the controller supplying power for each bunch⁵⁴⁵
 526 when it should not be adding any (note that maintenance of the⁵⁴⁶
 527 steady state point should not require power). Close comparison⁵⁴⁷
 528 of Figures 4 and 6 indicates that the set point is being over shot⁵⁴⁸
 529 during the bunch train; even so almost exactly the same voltage⁵⁴⁹
 530 is achieved in the mode for every bunch of the train. ⁵⁵⁰

531 Figure 9 shows identical voltage kicks applied to successive⁵⁵¹
 532 bunches. The steady state voltage kicks are slightly higher than⁵⁵²
 533 for the case with no active damping (Figure 3) and this is be-⁵⁵³
 534 cause unnecessary power was supplied. The kicks can be re-⁵⁵⁴
 535 duced to zero by altering the set point voltage and allowing a⁵⁵⁵
 536 higher power overhead to compensate the gaps. This case is⁵⁵⁶
 537 shown in Figure 10. Zero voltage kick was achieved with a set⁵⁵⁷
 538 point voltage of 3400 V. In order to achieve the set point with⁵⁵⁸

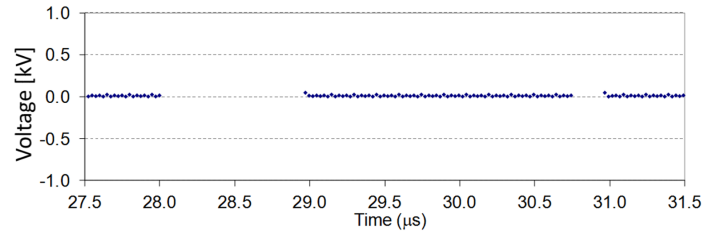


Figure 10: Bunch kicks using active control with gain = 1500, $Q_e = 100$, set point chosen to give zero kick.

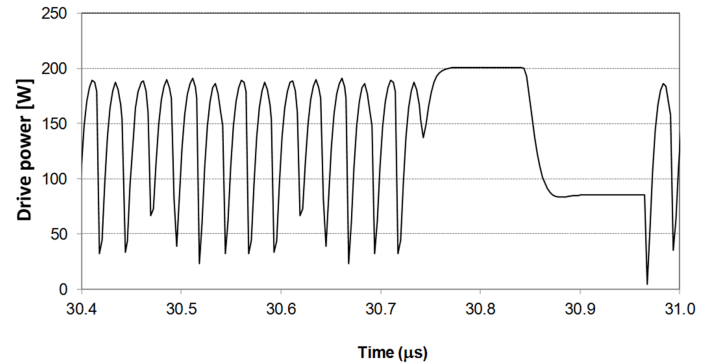


Figure 11: Drive power required for zero kick.

the same gain as before the power limit for the amplifier was increased to 200 W and the amplifier bandwidth was increased from 50 MHz to 70 MHz.

Figure 11 shows the power requirement for the voltage kicks associated with Figure 10. The power requirement to achieve zero kicks is slightly higher than that shown in Figure 8 where the intention had been to maintain the steady state point.

Control with minimal power during the bunch train can be obtained by reducing controller gain and amplifier bandwidth. Results when the gain is reduced by a factor of 5 and the amplifier bandwidth is reduced from 50 MHz to 15 MHz are shown in Figures 12-15. Drive power is shown in Figure 12, the first peak is at the start of a long gap of 38 missing bunches and the second peak is for a short gap of 8 missing bunches elsewhere during bunch trains the power is practically zero.

When the amplitude in Figure 13 is compared with the amplitude in Figure 6 it should be noted that Figure 13 has its time axis expanded around the short gap in the bunch train. During the bunch train Figure 13 shows the variation in the mode voltage to be reduced with respect to Figure 6, this is because no

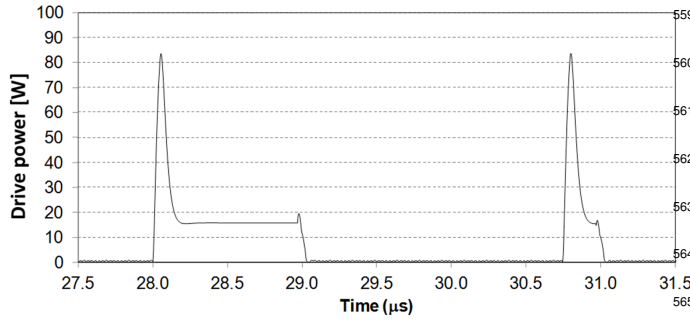


Figure 12: RF power at gain = 300, Amplifier bandwidth = 15 MHz, $Q_e = 100$.

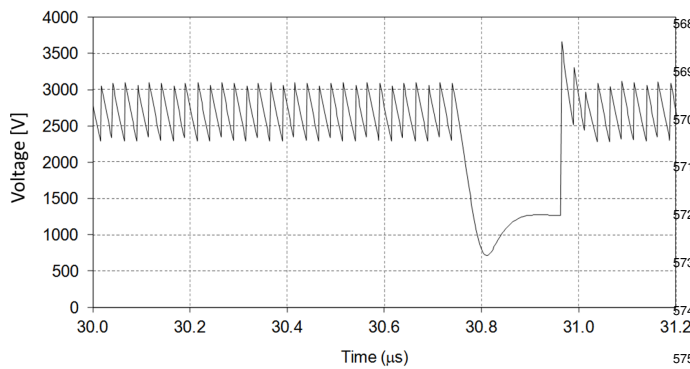


Figure 13: Mode amplitude for gain = 300, Amplifier bandwidth = 15 MHz, $Q_e = 100$.

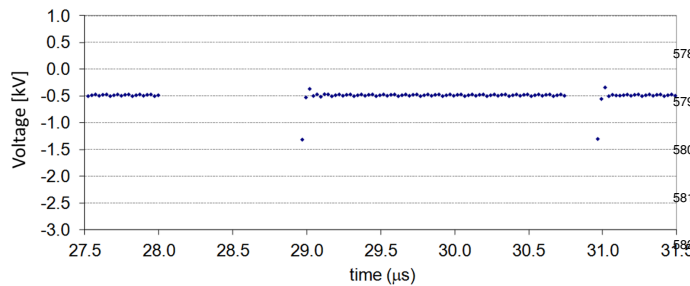


Figure 14: Bunch kicks for gain = 300, Amplifier bandwidth = 15 MHz, $Q_e = 100$.

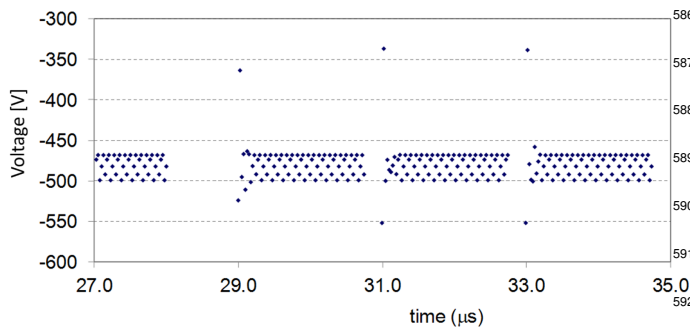


Figure 15: Same as Figure 14 but with expanded time axis to show the levels of voltage kick after transients have died away.

power is going into the mode. The variation in amplitude for Figure 13 is now similar to the case without control shown in Figure 4; except at the start of a train.

The resulting kicks shown in Figure 14 are much reduced at the start of the train as compared with Figure 3 but worse than in Figure 10 where compensation was almost perfect. It is likely that an optimal control scheme can be found which only applies power to the first few bunches and achieves identical kicks for every bunch. The easiest way to construct one is to reduce the gain during the bunch. It is of interest to show the kicks of Figure 14 on an expanded scale (Figure 15) which shows three distinct levels associated with the three phases.

Distinct levels arise whenever there are delays in the controller or averaging of measurements of the mode amplitude. Increasing the bandwidth for the measurements or increasing the integral term in the controller increases the splitting of these levels. As delays in the control system increase, the gain must be reduced to limit the splitting of these levels.

5. Active damping at resonance

When the acceleration mode is damped to a Q of 100 then the bandwidth of the mode is 3.7 MHz. During operation with a 25 ns bunch separation it is necessary that the mode never moves by 14 MHz to 360.72 MHz. More critically during operation with a 50 ns bunch separation it is necessary that the mode never shifts by 6.68 MHz to 380.76 MHz. It is desirable to reduce the damping of the acceleration mode by increasing the external Q factor from 100 to 300 or more to increase security against the mode ever being driven onto resonance. When the simulations of section 4 are repeated for an external Q factor of 300 the RF power must be increased to about 300 W for a similar control performance. The average voltage in the cavity remains at 2.7 kV but with less variation. The set point can be fixed to give zero voltage kick.

If one now considers the worst case scenario with 25 ns bunch separation where the unwanted acceleration mode moves to 360.72 Hz it is shown later in this section that active damping can limit the cavity voltage and the voltage kicks to an ac-

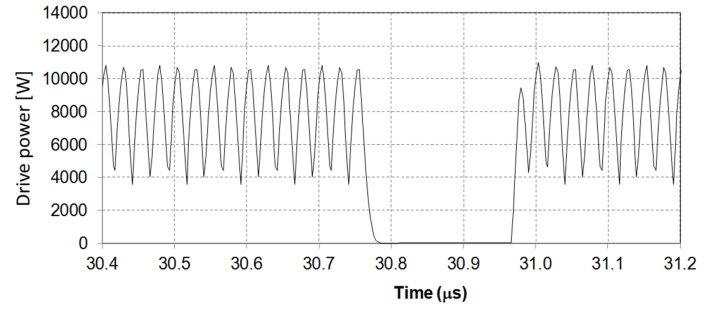
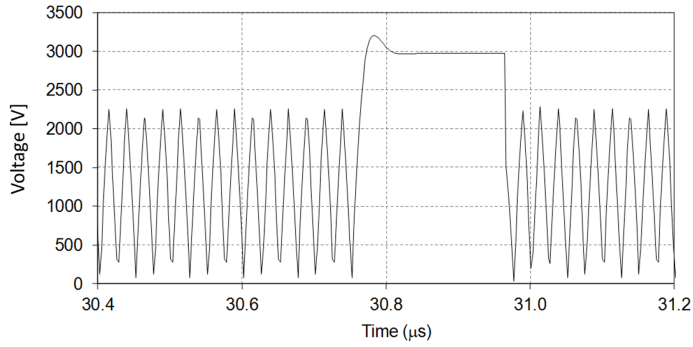


Figure 18: RF power on resonance for gain = 1500, $Q_e = 300$.

Figure 16: Mode voltage on resonance for gain = 1500, $Q_e = 300$. note that data sampling is not able to show amplitude dips extending to zero on phase reversal.

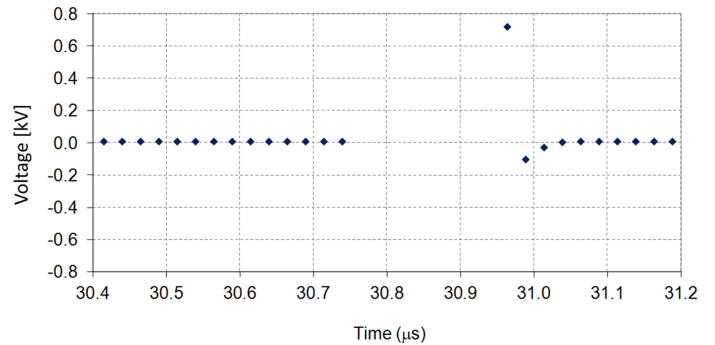
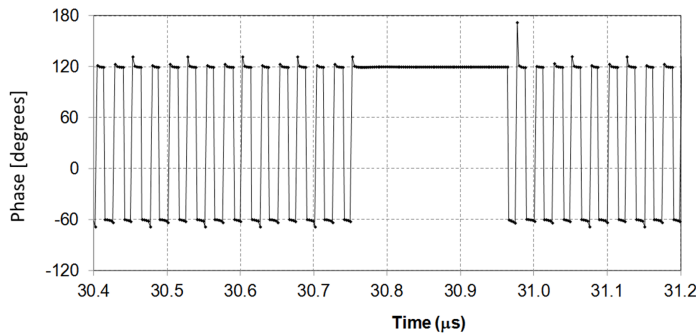


Figure 19: Bunch kicks on resonance for gain = 1500, $Q_e = 300$.

Figure 17: Mode phase on resonance for gain = 1500, $Q_e = 300$.

to 19 show that with active control that the voltage flips from 2 kV with a phase of 120° to 2 kV with a phase of -60° when a bunch arrives (i.e. the voltage reverses). Figure 16 shows amplitude, hence the flip at the voltage peak is not apparent. Power then drives the voltage back to its starting point and Figure 17 shows a second phase reversal as the voltage passes through zero. Figure 18 shows the power requirement for each bunch.

Figure 19 shows that the worst voltage kick for the first bunch is only 700 V compared to 50 kV without compensation. Importantly only 11 kW peak power is required to achieve this control whereas 30 kW of peak power flows out of the coupler in the absence of active control.

With active control at resonance the waveform on the coupler is almost a standing wave hence power out almost equals power in. The 11 kW required for active control on resonance can be reduced to 4 kW for an external Q factor of 100 but needs to be increased to 35 kW for an external Q factor of 1000. Running at resonance is probably academic as one would expect to be able to tune the mode away from resonance while warm during

ceptable level. For this case one no longer takes the set point voltage as the steady state voltage as determined by Eq. 11 as this is very high; instead a much smaller voltage is taken. For the simulation results presented in the following figures, Eq. 10 is used to provide the phase and the set point voltage is taken as 3140 V.

Figures 16, 17 and 18 plot mode voltage amplitude, mode phase and RF power respectively, on resonance with active damping using the same control parameters as used for the calculations presented in Figures 6 to 10 of section 4.

The power available from the amplifier was increased to 12.5 kW. In the absence of active control the mode voltage rises to 50 kV at the end of each bunch train and the peak power extracted from the beam is 30 kW. Other proposed crab cavity solutions for the LHC luminosity upgrade [8] (as opposed to the 4 rod cavity) would extract substantially higher power from the beam due to their higher monopole impedances. Figures 16

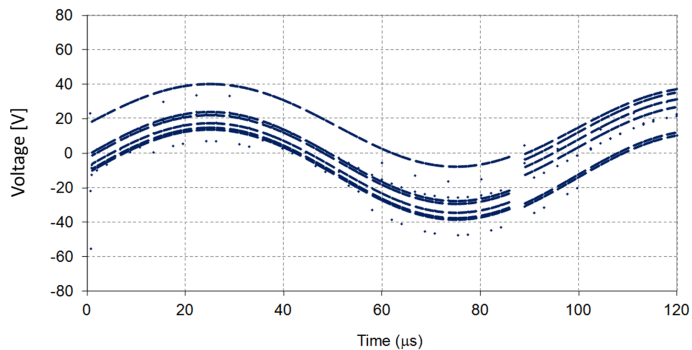


Figure 20: Active control with microphonics.

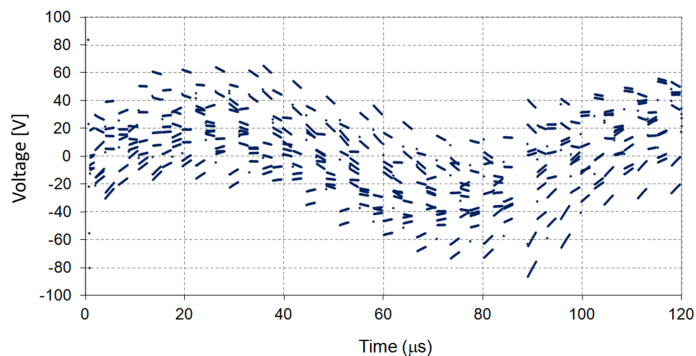


Figure 21: Effect of introducing an integral term in the controller with respect to Figure 20.

632 installation into the cryostat. This is not straightforward as suf-
 633 ficient testing on prototypes is required to understand frequency
 634 shifts of the LOM during cooling. It is important to realize that
 635 even at resonance the mode can be controlled with a modest
 636 amount of power for low external Q factors.

637 6. Mode detuning and measurement errors

638 An issue for superconducting cavities is control of phase and
 639 amplitude in the presence of microphonic detuning. The phase
 640 shift from detuning increases with loaded Q factor (Eq. 6) hence
 641 when the loaded Q is low as would be the case here, then huge
 642 frequency shifts are needed before the effect upsets the control
 643 system. Figure 20 shows kicks as a function of time when detuning
 644 with an amplitude of 200 kHz is introduced as a 10 kHz
 645 sinusoid. This amount of detuning would require a deflection
 646 of 0.1 mm to be applied to the cavity in its most sensitive di-
 647 mension. Note that the time scale plotted is much longer than
 648 the periods used in previous figures hence many trains of 72
 649 bunches are displayed.

650 The voltage axis scale is greatly expanded so that the split-
 651 ting of the steady state previously observed in Figure 15 can be
 652 seen. Detuning at the level of 200 kHz only perturbs the volt-
 653 age kicks by ± 40 V. In conventional LLRF control systems an
 654 integral term is introduced to eliminate tuning offsets. In this
 655 situation where the mode frequency is not an integer multiple
 656 of the bunch frequency an integral term gives no benefit to the
 657 controller. Figure 21 shows the effect of introducing a moderate
 658 integral term into the controller; resulting in a randomization of

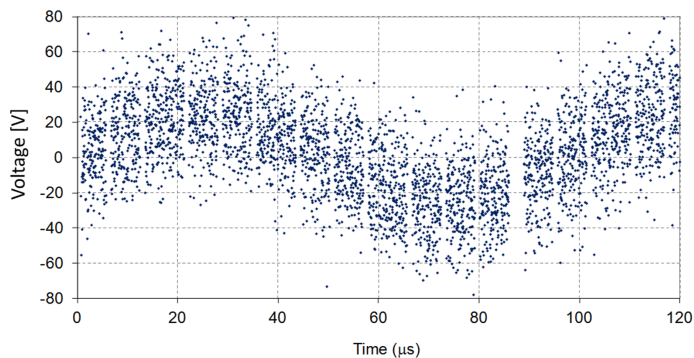


Figure 22: Effect of introducing measurement errors with respect to Figure 20.

the net kick to each bunch. Large integral terms always result
 in larger voltage kicks to bunches at the start of a train.

A key question for setting up the control system is the accu-
 racy of measurement of amplitude and phase required for the
 unwanted LOM. Figure 22 repeats the simulation of Figure 20
 with random phase and amplitude errors on the mode measure-
 ments. Specifically the phase error is taken as $\pm 5^\circ$ and the am-
 plitude error as $\pm 5\%$. The figure shows that even with huge
 measurement errors the random kicks are very small compared
 to the situation without active damping.

It is apparent in this system that performance is insensitive
 to measurement errors at a level significantly higher than one
 would normally expect for an accelerator system.

For the pure feed forward algorithm measurements are not
 needed once the charge in every bunch is known and one has
 a clock that is synchronous with the bunches, this is unless the
 mode frequency has shifted by a sizable fraction of its band-

676 width. If an element of feedback is to be included as secu-
 677 rity against large frequency shifts one might directly sample the
 678 voltage in the mode with 8 bit accuracy at several GHz.

679 7. Conclusions

680 This paper sets out a hitherto unexplored method using active
 681 damping to eliminate wakes from low order acceleration modes
 682 in dipole cavities; this could be for mode frequencies above or
 683 below the dipole operating mode. Control would need to be pri-
 684 marily by feed forward. A method for determining the feed for-
 685 ward drive power has been set out and performance with respect
 686 to minimizing momentum kicks has been determined. The sim-
 687 ulations have encompassed the complex LHC bunch structure
 688 and detuning. The paper shows that only a few hundred Watts
 689 of power is sufficient to eliminate the wake when the unwanted
 690 mode is far from resonance. In the event of a catastrophe mov-
 691 ing the mode onto resonance then 11 kW of power is required
 692 to eliminate the wake when the loaded Q factor is 300.

693 It should be noted that to damp multiple modes, a controller
 694 is required for each additional mode, but corrective power can
 695 be supplied by a single broadband amplifier.

696 Appendix - Simulation model

697 The frequency separation of the unwanted acceleration mode
 698 from the dipole operating mode allows it to be modeled as a sin-
 699 gle LCR oscillator as shown in Figure 23 where the transmis-
 700 sion line is the coupler used to damp the mode. At the terminal,
 701 the voltage in the transmission line of the coupler must equal
 702 the voltage in the lumped circuit. Along the entry transmission
 703 line (i.e. the power coupler) the voltage and current satisfies the
 704 wave equation.

705 The current on the transmission line is given as

$$706 I(z, t) = \frac{1}{Z_{wg}} \left[V_F e^{j(kz - \omega t)} - V_R e^{-j(kz + \omega t)} \right] \quad (13)$$

707 where

$$708 k = \omega \sqrt{L_{wg} C_{wg}}$$

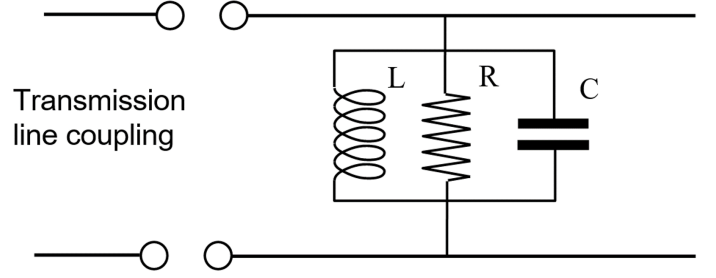


Figure 23: Equivalent circuit of an RF cavity.

$$Z_{wg} = \sqrt{\frac{L_{wg}}{C_{wg}}}$$

C_{wg} is the capacitance per unit length

L_{wg} is the inductance per unit length

V_F and V_R are the amplitudes of the forward and reflected voltage waves.

Taking the terminal between the cavity and the waveguide at $z = 0$ and the voltage in the cavity as V then

$$V = (V_F + V_R) e^{-j\omega t}. \quad (14)$$

The current in the transmission line equals the sum of the currents through the equivalent circuit components of each series resonator hence

$$\frac{1}{L_{wg}} \int V dt + C_{wg} \frac{dV}{dt} + \frac{V}{R} = \frac{V_F - V_R}{Z_{wg}} e^{-j\omega t}. \quad (15)$$

By substituting Eq. 14 into Eq. 15, one can eliminate the reflected voltage and obtain

$$\frac{1}{L_{wg}} \int V dt + C_{wg} \frac{dV}{dt} + \frac{V}{R} + \frac{V}{Z_{wg}} = \frac{2V_F}{Z_{wg}} e^{-j\omega t}. \quad (16)$$

This equation determines the modal voltages in the cavity as a function of the amplitude of the forward wave in the waveguide. Defining the natural frequency of the mode as $\omega_0 = 1/\sqrt{L_{wg} C_{wg}}$ then the definition of the intrinsic and external Q factors gives $Q_0 = \omega R C_{wg}$ and $Q_e = \omega Z_{wg} C_{wg}$ respectively hence

$$Z_{wg} = \left(\frac{R}{Q_0} \right)_C Q_e. \quad (17)$$

726 The suffix C is used to denote the circuit definition of R/Q .⁷⁴⁴
 727 Defining the loaded Q factor using

$$\frac{1}{Q_L} = \frac{1}{Q_0} + \frac{1}{Q_e} \quad (18)^{747}$$

728 then differentiation of Eq. 16 with the given definitions give
 729 the driven cavity equation as

$$\frac{d^2V}{dt^2} + \frac{\omega}{Q_L} \frac{dV}{dt} + \omega_0^2 V = \frac{2\omega}{Q_e} \frac{d}{dt} \{V_F e^{-j\omega t}\}. \quad (19)^{751}$$

730 In this equation ω is the RF drive frequency and ω_0 is the
 731 angular frequency for the mode in a lossless cavity.⁷⁵⁴

732 For resonant systems where Q factors are greater than about⁷⁵⁵
 733 30 one does not need to solve for the voltages at any instant,⁷⁵⁶
 734 it is sufficient to solve for the amplitude and phase. More con-⁷⁵⁷
 735 veniently than solving for amplitude and phase one solves for⁷⁵⁸
 736 in phase and quadrature components of the voltage. Here the⁷⁵⁹
 737 in phase part is denoted with the suffix r and the quadrature⁷⁶⁰
 738 path with the suffix i . The in phase and quadrature voltages A_r ,⁷⁶¹
 739 and A_i can be defined with respect to the RF master oscillator,⁷⁶²
 740 frequency ω as

$$V(t) = (A_r(t) + jA_i(t)) e^{-j\omega t}. \quad (20)^{765}$$

741 After making approximations consistent with a slowly vary-
 742 ing amplitude and phase, Eq. 19 can be replaced with the two
 743 first order differential equations as follows

$$\begin{aligned} & \left[\left(\frac{2\omega}{\omega_0} \right)^2 + \left(\frac{1}{Q_L} \right)^2 \right] \frac{1}{\omega_0} \dot{A}_r + \left(\frac{\omega^2}{\omega_0^2} + 1 \right) \frac{1}{Q_L} A_r + \\ & \left[\left(\frac{1}{Q_L} \right)^2 - 2 \left(\frac{\omega_0^2 - \omega^2}{\omega_0^2} \right) \right] \frac{\omega}{\omega_0} A_i = \\ & \frac{2}{Q_e Q_L} \left(\frac{1}{\omega_0} \dot{V}_{F,r} + \frac{\omega}{\omega_0} V_{F,i} \right) + \frac{4}{Q_e} \frac{\omega}{\omega_0} \left(\frac{1}{\omega_0} \dot{V}_{F,i} - \frac{\omega}{\omega_0} V_{F,r} \right) \end{aligned} \quad (21)^{766}$$

$$\begin{aligned} & \left[\left(\frac{2\omega}{\omega_0} \right)^2 + \left(\frac{1}{Q_L} \right)^2 \right] \frac{1}{\omega_0} \dot{A}_i + \left(\frac{\omega^2}{\omega_0^2} + 1 \right) \frac{1}{Q_L} A_i - \\ & \left[\left(\frac{1}{Q_L} \right)^2 - 2 \left(\frac{\omega_0^2 - \omega^2}{\omega_0^2} \right) \right] \frac{\omega}{\omega_0} A_r = \\ & \frac{2}{Q_e Q_L} \left(\frac{1}{\omega_0} \dot{V}_{F,i} - \frac{\omega}{\omega_0} V_{F,r} \right) + \frac{4}{Q_e} \frac{\omega}{\omega_0} \left(\frac{1}{\omega_0} \dot{V}_{F,r} + \frac{\omega}{\omega_0} V_{F,i} \right). \end{aligned} \quad (22)^{771}$$

The difference between solving Eq. 19 and the envelope
 equations (Eqs. 21 and 22) is that one no longer needs multi-
 ple time steps per RF cycle.

Beam loading is incorporated by allowing the phase and am-
 plitude of the cavity excitation to jump in proportion to the im-
 age charge deposited in the cavity after the passage of the bunch
 see Eqs. 2 and 3 in the main text.

A digital LLRF system typically measures in phase and
 quadrature components of the cavity fields and controls each
 component to a set point by varying the in phase and quadra-
 ture components of the RF input. Importantly the system is de-
 scribed by two first order differential equations rather than one
 second order differential system. The optimum controller for
 a first order system with random disturbances is a Proportional
 Integral (PI) controller. The code used here has a PI controller
 option but the integral term is not used for the reasons given
 in the main text. When disturbances are well understood better
 controllers can be devised.

For any cavity mode an issue with the control is whether one
 can determine its amplitude and phase. If one can and with
 reference to the envelope equations one determines the drive
 for a PI controller as

$$\begin{aligned} V_{F,r}(t + t_{delay}) &= c_p (A_{r,sp} - A_r) + c_i \left(\frac{\omega}{2\pi} \right) \int_{-\infty}^t (A_{r,sp} - A_r) dt \\ V_{F,i}(t + t_{delay}) &= c_p (A_{i,sp} - A_i) + c_i \left(\frac{\omega}{2\pi} \right) \int_{-\infty}^t (A_{i,sp} - A_i) dt \end{aligned} \quad (23)$$

where t_{delay} is the time it takes to measure the error and adjust
 the amplifier output, $A_{r,sp}$ and $A_{i,sp}$ are the in phase and quadra-
 ture voltage set points and c_p and c_i are the gain coefficients for
 the proportional and integral controllers respectively.

770 Acknowledgements

This work has been supported by STFC ST/G008248/1 and
 the European Union 7th Framework Program, grant number
 227579 EuCARD.

774 **References**

- 775 [1] O. Bruning, H. Burkhardt, S. Myers, *The Large Hadron Collider*, CERN-
776 ATS-2012-064, 2012
- 777 [2] B. Hall, G. Burt, C. Lingwood, R. Rimmer, H. Wang, *Novel Geometries*
778 *for the LHC Crab Cavity*, IPAC'10, Kyoto
- 779 [3] F. Zimmermann, *LHC upgrade scenarios*, Particle Accelerator Conference,
780 2007. IEEE, DOI: 10.1109/PAC.2007.4441113
- 781 [4] R. B. Palmer, *Energy scaling, crab crossing and the pair problem*, SLAC-
782 PUB-4707, 1988
- 783 [5] K. Akai et al., *RF systems for the KEK B-Factor*, Nucl.Instrum.Meth.
784 A499 (2003) 45-65
- 785 [6] Y. P. Sun, R. Assmann, J. Baranco, R. Tomas, T. Weiler, F. Zimmermann,
786 R. Calaga, A. Morita, *Beam Dynamics Aspects of Crab Cavities in the*
787 *LHC*, Phys. Rev. ST Accel. Beams 12, 101002 (2009)
- 788 [7] B. Hall, P. K. Ambattu, G. Burt, A. C. Dexter, D. Doherty, C. Lingwood,
789 R. Calaga, E. Jensen, R. Rimmer, H. Wang, D. Gorelov, T. Grimm, E.
790 Schnabel, P. Goudket, C. Hill, P. A. McIntosh, *Analysis of the four rod*
791 *crab cavity for HL-LHC*, IPAC'12, New Orleans
- 792 [8] J. R. Delayen, *Compact Superconducting Cavities for Deflecting and Crab-*
793 *bing Applications*, SRF Conference, 2011, Chicago
- 794 [9] F. Tamura, M. Yamamoto, C. Ohmori, A. Schnase, M. Yoshii, M. Nomura,
795 M. Toda, T. Shimada, K. Hara, K. Hasegawa, *Multiharmonic rf feedfor-*
796 *ward system for beam loading compensation in wide-band cavities of a*
797 *rapid cycling synchrotron*, Phys. Rev. ST Accel. Beams 14, 051004 (2011)
- 798 [10] D. K. Douglas, K. C. Jordan, L. Mermina, E. G. Pozdeyev, D. Tennant, H.
799 Wang, T. I. Smith, S. Sirock, I. V. Bararov, G. H. Hoffstaetter, *Experimental*
800 *investigation of multibunch, multipass beam breakup in the Jefferson Lab-*
801 *oratory Free Electron Laser Upgrade Driver*, Phys. Rev. ST Accel. Beams
802 9, 064403 (2006)
- 803 [11] A. Dexter, G. Burt, *Phase and Amplitude Control of Dipole Crabbing*
804 *Modes in Multi-Cell Cavities*, EUROTeV-Report-2008-064, 2008
- 805 [12] P. Baudreghien et al., *Functional Specifications of the LHC Prototype*
806 *Crab Cavity System*, CERN-ACC-NOTE-2013-003, 2013